

Phases of QCD — *Baryon Rich State of Matter* —

Kenji Fukushima

Yukawa Institute for Theoretical Physics, Kyoto University, Kyoto 606-8502, Japan

E-mail: fuku@yukawa.kyoto-u.ac.jp

Abstract. Recent topics in the research of phases of QCD are reviewed. The possibility of separate QCD phase transitions, the appearance of the quarkyonic phase and the associated triple point structure, the existence of the QCD critical point, and some model analysis are discussed.

1. Introduction

Quantum Chromodynamics (QCD) is the fundamental theory of the strong interactions. It is a long standing problem to explore the phase diagram of QCD at finite temperature T and baryon density n_B (or baryon chemical potential μ_B or quark chemical potential $\mu_q = \mu_B/N_c$ in the grand canonical ensemble) [1]. In the perturbative calculation of QCD a mass scale arises through the trace anomaly and the dimensional transmutation. This scale parameter Λ_{QCD} gives the typical energy scale of QCD physics. The running of the strong coupling constant $\alpha_s(Q)$ is determined in the perturbative QCD (pQCD) analysis of various high-energy processes, from which $\Lambda_{\text{QCD}} \sim 200$ MeV is estimated (but the precise value depends on the renormalization scheme of the pQCD analysis). Thus, the temperature and the density of our interest in connection to the QCD phase diagram are both characterized by Λ_{QCD} ; a state of hot QCD matter at $T \gtrsim \Lambda_{\text{QCD}}$ is a quark-gluon plasma (QGP). Until a couple of decades ago it had been considered that extremely dense QCD matter would be a QGP too unless the temperature is many orders of magnitude smaller than Λ_{QCD} . It has been recognized later that the gap energy Δ of a color superconducting (CSC) state is comparable to Λ_{QCD} and thus the QCD phase diagram must have a complicated structure with substantial regions of many CSC variants [2].

Figure 1 shows a structure of the QCD phases that satisfies minimal requirements from theoretical knowledge based on pQCD analysis. Properties of QCD matter in the region at $T > \Lambda_{\text{QCD}}$ and $\mu_B \ll T$ have been well investigated by pQCD calculations (in the hard thermal loop approximation) as well as by lattice-QCD simulations. The notion of the strongly-correlated QGP (sQGP) is also established in this region from the analysis of the data taken at Relativistic Heavy-Ion Collider (RHIC). [Note that sQGP does not necessarily mean a system at infinitely strong coupling constant, though large α_s is sometimes assumed.] Theoretical and experimental efforts along this direction are continuing into the next generation collider, i.e. Large Hadron Collider (LHC).

On the other hand, theoretical researches at high baryon density, $\mu_B \gtrsim T$, are facing a difficult situation. There is no doubt about the existence of the CSC phase, particularly a three-flavor symmetric state called the color-flavor locked (CFL) phase, at extremely high density where the strange quark mass effect is negligible ($\Delta \gg m_s^2/\mu_q$). In the so-called intermediate

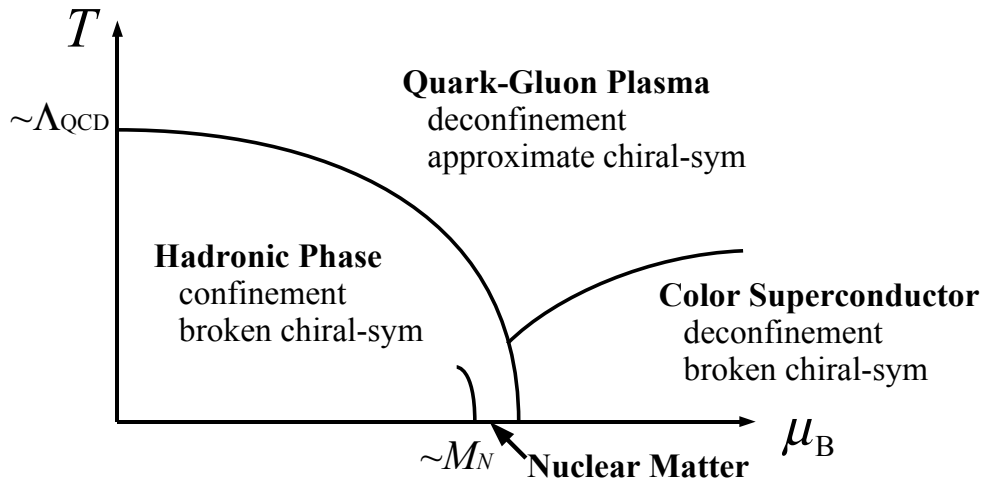


Figure 1. Minimal structure of the QCD phases in the μ_B - T plane. The critical temperature is of order Λ_{QCD} and the critical chemical potential is near the nucleon mass (minus the nuclear binding energy) which is of order $N_c \Lambda_{\text{QCD}}$.

density region with $\Delta \sim m_s^2/\mu_q$, many pairing patterns with respect to color, flavor, spin, etc become competing and it is still an unanswered question what the ground state should be then. There are several major reasons why the high-density direction is harder to explore than the temperature. First of all, the lattice-QCD simulation is of no practical use because of the sign problem and no guiding principle is available from numerical experiments unlike the finite- T case. Second of all, the heavy-ion collision has only a faintest chance to probe the properties of cold and dense quark matter. The neutron star is another experimental candidate, but its structure is a superposition of various states of matter with different baryon density as a function of the radius. The information from the mass-radius relation is rather indirect. Finally, the theoretical treatment of baryons is far more involved than that of mesons, which causes substantial ambiguities in the model-type studies.

When we pose a question of some new phenomena between the experimentally accessible sQGP region and the theoretically founded CSC region, in my opinion, the situation in research on the QCD phase diagram may be reminiscent of the physics beyond the Standard Model. The Standard Model has been successfully established by getting through experimental tests, while the Planck scale is too far from reachable by any laboratory experiment. The idea of new physics comes from a challenge to the “energy desert” until the Planck scale, and the LHC is expected to give us some hints to new physics and how this extraordinary big energy scale can be compensated, for example by the compactification size of the extra dimension, down to the TeV scale. In a similar sense, there are lots of theoretical and experimental activities and challenges recently to fill the “desert” on the QCD phase diagram between the small- μ_B and the extremely large- μ_B regions.

As already mentioned, the RHIC at Brookhaven National Laboratory (BNL) has been conducting the heavy-ion collision program since the year of 2000, which will continue at higher collision energies at LHC where the heavy-ion collision is planned in the fall of 2010. At the same time, there are several future plans about the heavy-ion experiment at lower energies with the aim to find something new toward the higher- μ_B region. In addition to the low-energy scan program at RHIC already performed in early 2010, the Compressed Baryonic Matter (CBM) experiment at Facility for Antiproton and Ion Research (FAIR) and the Nuclotron-based Ion Collider Facility (NICA) at Joint Institute for Nuclear Researches (JINR) are competing

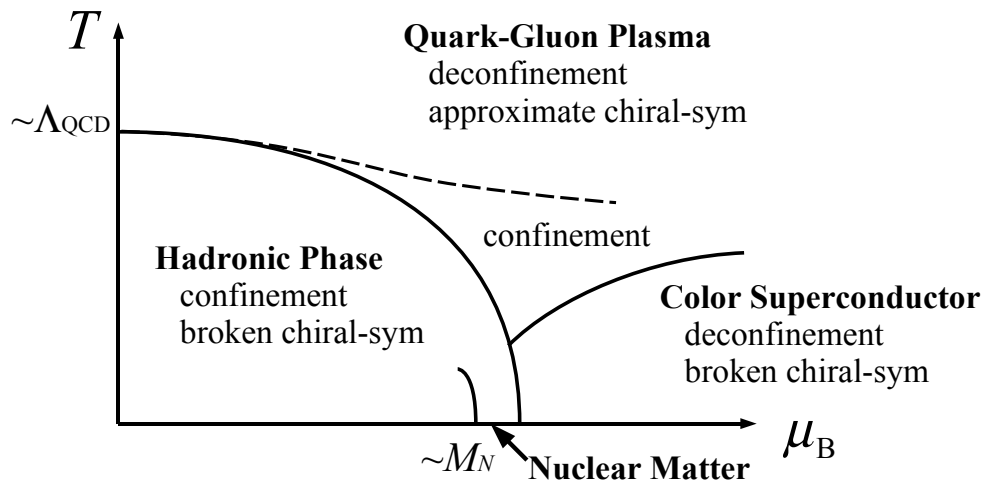


Figure 2. Minimal extension of the QCD phase diagram in the μ_B - T plane. It is logically possible that there appears a new window in which quarks are still confined and chiral symmetry is either restored or broken somehow in a different way from the hadronic phase.

candidates and will hopefully start the operation for the low-energy heavy-ion program around the year of 2013–2017. Here, in this article, some theoretical prospects of acquiring a new insight in the baryon rich state of QCD matter shall be summarized.

2. Chiral Symmetry Restoration and Quark Deconfinement

In Fig. 1 each phase is characterized by two features; whether quarks are confined or deconfined and whether chiral symmetry is spontaneously broken or restored. The QCD phase transitions associated with quark deconfinement and chiral symmetry restoration are associated with two global symmetries of QCD; *center symmetry* and *chiral symmetry*. The order parameter for quark deconfinement is the Polyakov loop $\ell = e^{-f_q/T}$ where f_q is the energy gain with a static charge placed in a hot gluonic medium. If $f_q \rightarrow \infty$ in the confined phase, $\ell \rightarrow 0$ and the system is center symmetric. Otherwise ($f_q < \infty$), center symmetry is broken by a finite value of the order parameter, i.e. $\ell \neq 0$. On the other hand, the order parameter for chiral restoration is the chiral condensate $\langle \bar{\psi}\psi \rangle$. Because $\bar{\psi}\psi$ is an operator conjugate to the quark mass, $\langle \bar{\psi}\psi \rangle \neq 0$ leads to a dynamical mass for quarks and chiral symmetry is spontaneously broken.

Since there are two independent criteria, four different phases should be possible, one of which is missing in Fig. 1. That is, Fig. 1 does not accommodate a state with quark confinement and (approximately) restored chiral symmetry. This is believed so without any field-theoretical proof, while a phenomenological argument would disfavor such a state [3, 4]. Let us think of a composite object which confines massless quarks with a *s*-wave potential. Massless quarks are eigenstates of chirality; right-handed quarks have the spin parallel to the momentum and left-handed quarks have the spin anti-parallel to the momentum and they do not mix together. Because quarks are localized inside the object, the momentum direction must be changed by the potential but the spin is not flipped. This means that quarks must change their chirality, which is possible only if chiral symmetry is broken. Hence, if this intuitive argument holds for any μ_B and T , such a state with confinement and restored chiral symmetry would be ruled out. This argument is, however, based on a potential model description and it is difficult to justify it from the first-principle argument.

Apart from the phenomenological potential model, no theory can exclude the phase structure as depicted in Fig. 2. The dashed curve represents a phase boundary associated with quark

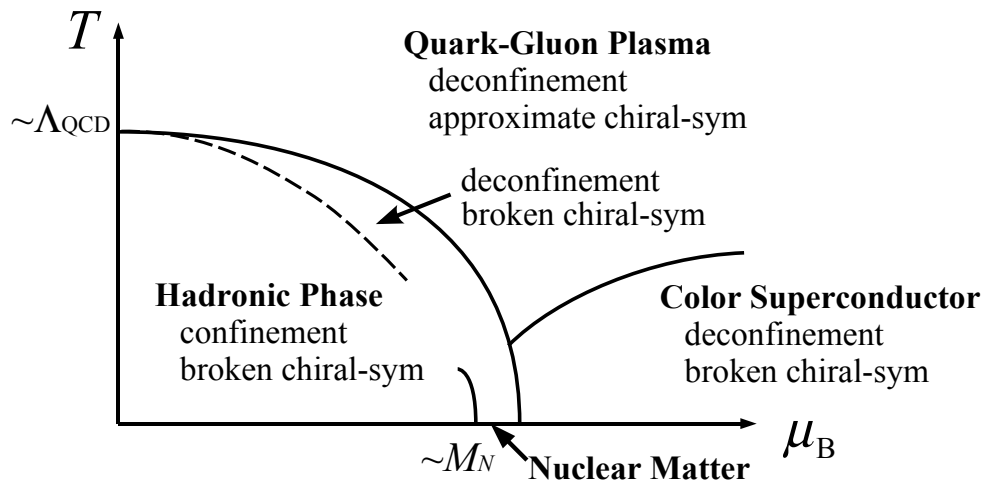


Figure 3. Another minimal extension of the QCD phase diagram in the μ_B - T plane.

deconfinement transition or crossover, below which quark confinement remains. To have distinction from the hadronic phase, chiral symmetry in the new window surrounded by the dashed and the solid curves should be either restored or broken somehow in a different way from the hadronic phase. As we will mention later, QCD at large N_c would favor this type of the phase structure with the new phase of so-called *quarkyonic matter* [5]. The identification of the chiral symmetry breaking pattern in quarkyonic matter is one of important issues under intense discussions [6].

Although there seem to be not many discussions about this, another possibility as illustrated in Fig. 3 is also likely to be the case in nature. This scenario is consistent with the phenomenological argument in the potential model description; the chiral phase transition occurs later than quark deconfinement. Therefore, in the region surrounded by the dashed and the solid lines in Fig. 3, chirally broken (dynamically heavy) quarks are deconfined.

As explained, the phase diagram of Fig. 2 is supported by large- N_c QCD and some of chiral model results. In contrast to this, the phase diagram of Fig. 3 is relatively minor, but preferred as well in some approaches. Actually the deconfinement transition takes place in the chiral broken phase if μ_B is finite, which is a good news for a successful description of the thermal Statistical Model [7, 8, 9]. In this model the nature of deconfinement is captured through Hagedorn's picture but any influence from the change of chiral properties is taken into account. Regarding the chiral sector the phase transition occurs with quark degrees of freedom, which would validate the model description by means of quark models such as the Nambu–Jona-Lasinio (NJL) model and its variants [10]. Anyway, there is no convincing reason why one of Figs. 2 and 3 is more preferable than the other.

3. Quarkyonic Matter and Triple Point

Recently an interesting possibility about the new structure of the QCD phase diagram has been suggested from analytic considerations on the large- N_c limit of QCD at finite T and μ_B [5]. The phase diagram takes a simple structure as sketched in Fig. 4 with three phases separated by the first-order phase transitions.

Let us first look at the phase transition of large- N_c QCD at $\mu_B = 0$. As long as quarks and gluons are confined, the hadronic phase has only glueballs and mesons which lead to the system pressure of $O(N_c^0)$, while the pressure increases up to $O(N_c^2)$ in the deconfined phase because of the presence of $N_c^2 - 1$ gluons released in the deconfined phase. Because the pressure

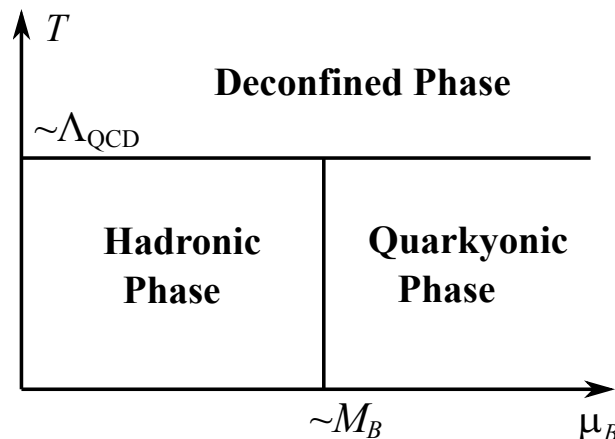


Figure 4. The phase diagram of large- N_c QCD [5]. The hadronic phase confines colored excitations and only glueballs and mesons exist and thus the system pressure is of $O(N_c^0)$. Above the deconfinement temperature of order of Λ_{QCD} , thermal excitations are dominated by gluons and the associated pressure is of $O(N_c^2)$. The quarkyonic phase is characterized by the pressure of $O(N_c)$ at μ_B greater than the lightest baryon mass M_B .

suddenly jumps from $O(N_c^0)$ to $O(N_c^2)$, the phase transition is likely to be of first order (though a continuous phase transition is still possible).

Next, we think of the effect of finite μ_B . In the large- N_c limit quark loops are always suppressed by $1/N_c$ as compared with gluon loops, so μ_B does not affect the deconfinement transition line which is predominantly determined by $N_c^2 - 1$ gluons. Hence the deconfinement transition makes a straight line parallel to the μ_B axis. A free quark gas would give a pressure of $\sim N_c \mu_q^4 \sim N_c^{-3} \mu_B^4$, and thus the deconfinement transition line would be deformed for μ_B as large as $O(N_c^{5/4})$. Before this is reached, there appears another type of transition at $\mu_B \simeq M_B$ where M_B is the lightest baryon excitation energy (baryon mass minus binding energy). The baryon number density n_B becomes non-vanishing then and the system pressure jumps from $O(N_c^0)$ in the hadronic phase to $O(N_c)$ in the new phase which is called the quarkyonic phase. Before the deconfinement phase transition takes place with $T \sim \Lambda_{\text{QCD}}$, glueballs and mesons cannot affect this threshold for the baryon number and so the threshold located at $\mu_B \simeq M_B$ makes a straight line parallel to the T axis, which results in the phase structure presented in Fig. 4 after all.

The reason why the right-bottom region is named the quarkyonic phase is the following. As explained before, quarks and gluons are all confined below the deconfinement transition line, and so the quarkyonic phase region resides in the confined region. Therefore the physical degrees of freedom there should be baryons rather than quarks, and one can show that the dense baryonic system at large N_c indeed gives the pressure of $\sim O(N_c)$ whose major contribution comes from the baryon-baryon interaction energy [5]. On the other hand, a gas of quarks naturally yields a pressure of $O(N_c)$ because of the presence of N_c quarks. Such N_c counting implies that this bottom-right state would confine quarks and nevertheless feel quarks somehow (i.e. quark + baryonic phase = quarkyonic phase). This may sound peculiar but there is a reasonable way to reconcile two interpretations in terms of baryons and quarks. That is, particles sitting deeply inside the Fermi sea cannot be a part of excitation spectra, and so they could be quarks even though the system is in the confined phase. Therefore, the Fermi sphere consists of both baryons and quarks; baryons in the momentum layer $\sim \Lambda_{\text{QCD}}$ near the Fermi surface (but, because of the confining interaction, there is no sharp Fermi surface in reality) and quarks inside the Fermi

sphere which does not take part in the excitation but gives the pressure of $\sim O(N_c)$.

Remembering the possible extension illustrated in Fig. 2, one would be aware that the structure of Fig. 2 looks similar to the large- N_c phase diagram in Fig. 4. There is a difference, however; the vertical line in Fig. 4, on the one hand, represents the threshold where the baryon density suddenly increases and, on the other hand, the vertically stretching curve in Fig. 2 represents the chiral phase transition where $\langle\bar{\psi}\psi\rangle$ becomes vanishingly small. These are apparently distinct criteria, and nevertheless, they can be linked in a quasi-particle picture. When $\langle\bar{\psi}\psi\rangle$ gets smaller, the dynamical quark mass becomes smaller, so that the quark (or baryon) density increases. In this way, one can approximately identify the physical contents of Figs. 2 and 4.

It is a non-trivial question how to detect (any remnant of) the quarkyonic phase in the heavy-ion experiment. This is difficult to answer because the definition of the quarkyonic phase is not clear at all for finite N_c and we should keep in mind that $N_c = 3$ in nature is not a very large number. One interesting implication from the phase structure in Fig. 4 is the existence of the triple point where three phases meet (around $T \sim \Lambda_{\text{QCD}}$ and $\mu_B \sim M_B$).

Interestingly enough, in the thermal Statistical Model analysis, a region that might be regarded as the triple point has been found [11]. The chemical freeze-out curve is well examined in terms of the Statistical Model interpretation of the experimental data, namely the abundance of observed particles. It is easy to estimate within the framework of the Statistical Model how much mesons and how much baryons the thermodynamic quantities result from, respectively, along the chemical freeze-out curve. Then, it was found that the baryon contributions quickly overcome the mesonic ones around $\mu_B \sim 400$ MeV which may be interpreted as a point where the quarkyonic phase is activated. At finite baryon density K^+ (which contains a u -quark) is enhanced, whose strangeness carried by \bar{s} should be compensated by strange baryons like Λ . Thus, the properties of K^+ might be sensitive to the triple point-like region, and indeed, an abnormal horn structure has been observed in K^+/π^+ as a function of the center-of-mass energy (or the chemical potential μ_B) and its location happens to be close to $\mu_B \sim 400$ MeV [11].

4. Chiral Critical Point

Going back to the phase diagram for $N_c = 3$, it is of great importance what the order of the phase transition is. By now it has been almost established that the QCD phase transition at $\mu_B \ll T$ is smooth crossover [12]. There is no strong argument from theory for the finite- μ_B case, though. It may remain crossover, or may become discontinuous of first order. Model studies suggest that the first-order phase transition could be favored with increasing μ_B [13, 14, 15]. Here let us assume that the chiral phase transition turns to be of first order beyond some chemical potential. Then, an exact second-order phase transition point appears at the terminal of the first-order phase boundary (see Fig. 5).

There are lots of theoretical works on the properties of the chiral critical point. This is because the exact second-order phase transition and its critical phenomena do not depend on microscopic details of the underlying theory and one can develop rather model-independent analysis using the theory of critical phenomena in general [16, 17]. In the low-energy scan program in the heavy-ion experiments, multi-particle fluctuations of baryons such as the susceptibility, the Kurtosis, and the skewness [18] are being measured at various energies. If a non-monotonic bump is observed, it would be a signal for the QCD critical point.

However, one should always bear in mind that the existence, the location, and the width of the critical region are all model dependent. Thus, the physics of the QCD critical point strongly relies on the model-dependent starting point, even though the critical properties do not. To get rid of model-dependent assumptions, some first-principle calculations by the lattice-QCD simulation would be indispensable. Unfortunately, however, the lattice-QCD simulation does not work at finite baryon density due to the sign problem [19]. There are some suggestive

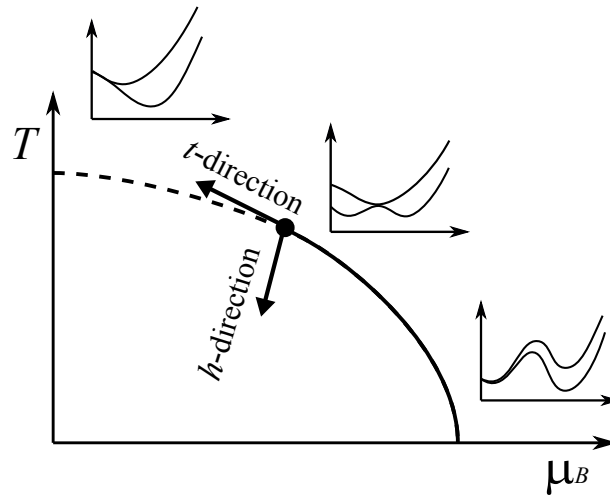


Figure 5. Chiral critical point and the associated change of the effective potential for the chiral order parameter. The tangential direction to the first-order curve preserves the Z_2 symmetry and can be identified as the temperature direction in the Ising model if the long-range effective theory is mapped onto the Ising model.

indications from recent lattice-QCD results, but it is not quite conclusive about whether the QCD critical point really exists or not.

Among various algorithms to circumvent the sign problem the multi-parameter reweighting method [20] is the best strategy in my opinion, but is most expensive. It is not obvious whether the Taylor expansion is useful for the purpose of the critical point search because the Taylor expansion method is only an approximate evaluation of the single-parameter reweighting (Glasgow) method [21] and it is unlikely that the Glasgow method can simply access the critical point. The canonical ensemble approach is an interesting possibility [22, 23], but the volume size is too small so far. One of the most important issues is the finite- μ_B evolution of the Columbia diagram, which has been investigated in the imaginary chemical potential method, and the result seems to disfavor the existence of the critical point [24]. Since results from various different approaches are not quite converging but rather inconsistent or even contradictory to each other, one should not put any intentional bias on preferable lattice-QCD output at present.

Before closing this section, it would be worth mentioning on further complication in the vicinity of the first-order phase transition. It is known that the susceptibility diverges not only at the second-order critical point but also along the spinodal instability lines [25], which may change the scenario of the non-monotonic behavior of the fluctuations in order to detect the critical point. More recently it is argued that the Lifshitz point (associated with spatially inhomogeneous condensates) coincides with the critical point in some chiral models [26]. The exact coincidence is a model-dependent consequence, but none the less, it is conceivable that the critical point and the critical region are all hidden beneath the transition to an inhomogeneous ground state such as the chiral density-wave state [27, 28] and the quarkyonic spiral state [6].

5. Some Model Analysis

Finally let us take a look at an example of the QCD phase diagram from recent model analysis. The existence and the location of the QCD critical point are furiously dependent on the model setup. In fact, reduction of the instanton-induced interaction strength would make the whole chiral phase transition be smooth crossover [30]. Likewise, the repulsive vector interaction would

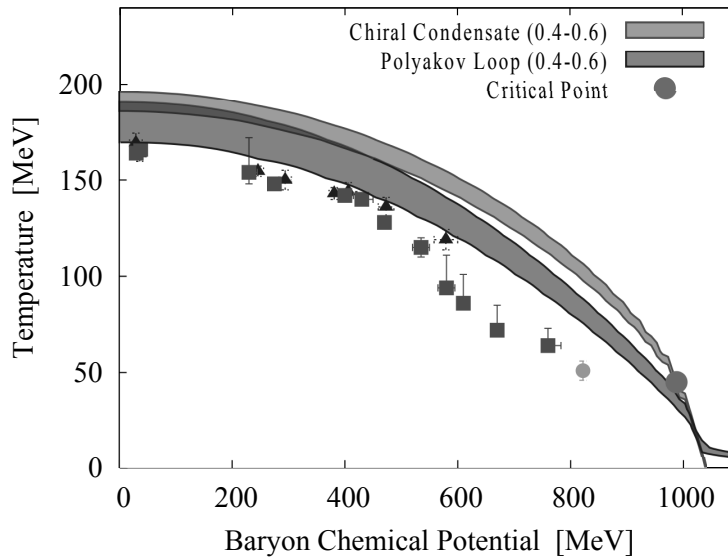


Figure 6. Phase diagram from a chiral model with the Polyakov loop coupling [31]. The chiral phase transition, the deconfinement transition and the chemical freeze-out points stay close to each other in this example.

easily let the critical point out of the QCD phase diagram [15, 29, 30].

Figure 6 shows two bands on top of the chemical freeze-out points [31]. One (slightly upper) band represents the region where the chiral condensate $\langle\bar{\psi}\psi\rangle$ normalized by the vacuum value ranges from 0.4 to 0.6, and the other (slightly lower) band represents the region where the Polyakov loop ℓ ranges from 0.4 to 0.6. The calculation is done in the mean-field approximation in the three-flavor NJL with the Polyakov loop coupling (PNJL model [32, 33]). It should be noted that the mean-field analysis is not a bad approximation for the bulk properties of the phase structure and the thermodynamics. If the QCD critical point is concerned, however, one should go beyond the mean-field analysis and make use of the renormalization group improvement [34, 35].

The most serious difficulty in the QCD phase diagram research lies in the fact that reliable data from experiments and/or first-principle calculations is quite limited. Without imposing any constraint, the model study badly suffers from ambiguities in the choice of the model parameters. Among others, in my thought, the chemical freeze-out points and the Statistical Model outputs could give us quantitative information about the baryon-rich state of QCD matter. As mentioned before, the chemical freeze-out points are plotted in Fig. 6, which are inferred from the thermal Statistical Model. The question is then how to cope with the order parameters, $\langle\bar{\psi}\psi\rangle$ and ℓ , which are missing in the Statistical Model setup. Recently an idea was proposed to constrain the PNJL model with the thermodynamic properties from the Statistical Model. The phase diagram in Fig. 6 is drawn in such a way that the PNJL model is adjusted to match up with the Statistical Model or more specifically the THERMUS results [36]. So far, to the best of my knowledge, Fig. 6 is the only phase diagram in which the consistency with the THERMUS and the chemical freeze-out points is taken into account. It is intriguing to point out that this phase diagram is of the type of Fig. 3 in contrast to the standard PNJL result of the type of Fig. 2 [29, 30, 37].

Because the research field of the QCD phase diagram is not already developed but still developing, it is impossible to conclude the article with any firm statement about the phase structure. Nevertheless, there is one thing that one can say with enough confidence. That is,

as explained in Introduction, more and more systematic experimental data is being taken at RHIC and also at FAIR and NICA in the near future. Then, some of model ambiguities shall be removed by the experimental constraints.

References

- [1] See; K. Fukushima and T. Hatsuda, arXiv:1005.4814 [hep-ph] and references therein.
- [2] See; K. Rajagopal and F. Wilczek, arXiv:hep-ph/0011333; M. G. Alford, A. Schmitt, K. Rajagopal and T. Schafer, Rev. Mod. Phys. **80**, 1455 (2008).
- [3] A. Casher, Phys. Lett. B **83**, 395 (1979).
- [4] P. Castorina, R. V. Gavai and H. Satz, arXiv:1003.6078 [hep-ph].
- [5] L. McLerran and R. D. Pisarski, Nucl. Phys. A **796**, 83 (2007).
- [6] T. Kojo, Y. Hidaka, L. McLerran and R. D. Pisarski, Nucl. Phys. A **843**, 37 (2010).
- [7] J. Cleymans, H. Oeschler, K. Redlich and S. Wheaton, Phys. Rev. C **73**, 034905 (2006).
- [8] F. Becattini, J. Manninen and M. Gazdzicki, Phys. Rev. C **73**, 044905 (2006).
- [9] A. Andronic, P. Braun-Munzinger and J. Stachel, Phys. Lett. B **673**, 142 (2009) [Erratum-ibid. B **678**, 516 (2009)].
- [10] T. Hatsuda and T. Kunihiro, Phys. Rept. **247**, 221 (1994).
- [11] A. Andronic *et al.*, Nucl. Phys. A **837**, 65 (2010).
- [12] Y. Aoki, G. Endrodi, Z. Fodor, S. D. Katz and K. K. Szabo, Nature **443**, 675 (2006).
- [13] M. Asakawa and K. Yazaki, Nucl. Phys. A **504**, 668 (1989).
- [14] A. Barducci, R. Casalbuoni, S. De Curtis, R. Gatto and G. Pettini, Phys. Lett. B **231**, 463 (1989).
- [15] K. Fukushima, Phys. Rev. D **78**, 114019 (2008).
- [16] M. A. Stephanov, K. Rajagopal and E. V. Shuryak, Phys. Rev. Lett. **81**, 4816 (1998).
- [17] Y. Hatta and T. Ikeda, Phys. Rev. D **67**, 014028 (2003).
- [18] M. A. Stephanov, Phys. Rev. Lett. **102**, 032301 (2009).
- [19] S. Muroya, A. Nakamura, C. Nonaka and T. Takaishi, Prog. Theor. Phys. **110**, 615 (2003).
- [20] Z. Fodor and S. D. Katz, JHEP **0203**, 014 (2002).
- [21] I. M. Barbour [UKQCD Collaboration], Nucl. Phys. A **642**, 251 (1998).
- [22] S. Ejiri, Phys. Rev. D **77**, 014508 (2008).
- [23] A. Li, X. Meng, A. Alexandru and K. F. Liu, PoS **LATTICE2008**, 178 (2008).
- [24] P. de Forcrand and O. Philipsen, PoS **LATTICE2008**, 208 (2008).
- [25] C. Sasaki, B. Friman and K. Redlich, Phys. Rev. Lett. **99**, 232301 (2007).
- [26] D. Nickel, Phys. Rev. Lett. **103**, 072301 (2009).
- [27] E. Shuster and D. T. Son, Nucl. Phys. B **573**, 434 (2000).
- [28] E. Nakano and T. Tatsumi, Phys. Rev. D **71**, 114006 (2005).
- [29] C. Sasaki, B. Friman and K. Redlich, Phys. Rev. D **75**, 074013 (2007).
- [30] K. Fukushima, Phys. Rev. D **77**, 114028 (2008) [Erratum-ibid. D **78**, 039902 (2008)].
- [31] K. Fukushima, arXiv:1006.2596 [hep-ph].
- [32] K. Fukushima, Phys. Lett. B **591**, 277 (2004).
- [33] C. Ratti, M. A. Thaler and W. Weise, Phys. Rev. D **73**, 014019 (2006).
- [34] V. Skokov, B. Friman, E. Nakano, K. Redlich and B. J. Schaefer, Phys. Rev. D **82**, 034029 (2010).
- [35] T. K. Herbst, J. M. Pawłowski and B. J. Schaefer, arXiv:1008.0081 [hep-ph].
- [36] S. Wheaton and J. Cleymans, Comput. Phys. Commun. **180**, 84 (2009).
- [37] L. McLerran, K. Redlich and C. Sasaki, Nucl. Phys. A **824**, 86 (2009).